Geotechnical Engineering Journal of the SEAGS & AGSSEA Vol. 45 No.2 June 2014 ISSN 0046-5828

Model Loading Tests on Bearing Behaviour of a Group Pile and Ground Deformation in Sand

S. Aoyama[1], B. Liu[2], L. Danardi[3], W. Mao[4], S. Goto[5] and I. Towhata[6]
Civil Engineering Department, The University of Tokyo, Tokyo, Japan
E-mail: aoyama@geot.t.u-tokyo.ac.jp

ABSTRACT: Model loading tests were conducted in dry sand to investigate the mechanism of pile-soil-pile interaction under group pile loading. The group pile was constituted of 9 (3×3) closed-end piles when the spacing between pile centres were 2.5 times of the pile diameter (2.5D) and 5.0 times (5.0D). The results showed that (1) yielding settlement of 2.5D group pile was larger than that of 5D group pile, (2) the subgrade reaction of the 2.5D group pile became less than that of the 5.0D group pile or a single pile when the load-settlement relationship was linear; (3) subgrade reactions of 2.5D and 5.0D group pile became similar after yielding of bearing load. Ground deformation was studied using with visualising tests and PIV analysis. It was shown that the ground deformation occurred as a block in case of 2.5D group pile and the deformed area expanded deeper as compared with 5.0D group pile. This mode of ground deformation reduced the subgrade reaction in 2.5D group pile.

Keywords: Group Pile, Model test, Vertical Load, Visualizing

1. INTRODUCTION

The behavior of a group pile is different from the summation of single piles if the spacing of pile becomes narrow enough because of pile-soil-pile interaction. To investigate the effects of the interaction for vertical resistance of the group pile, some studies have been conducted. The field tests such as Yu (2011) and Endo et al. (1980) suggested that the bearing capacity of the group pile becomes smaller than the summation of a single pile. Moreover, the load distribution in each pile was not uniform among pile members. The non-uniformity was different among the studies. Yu (2011) reported the corner pile carries more load. On the other hand, Endo et al. (1980) suggested that the center pile carried more load and the center pile was designed in larger diameter for the larger load. The difference would be caused by the variety of the stratum.

To investigate the mechanism of the interaction, model tests have been conducted in clayey or sandy ground. Whitaker (1957) conducted loading tests of the group pile in clayey ground and showed that bearing capacity of the group pile became smaller than the summation of the bearing capacity of single piles. And the corner piles carried more load than the center pile. From these results a block failure was assumed for the group pile in clayey ground when the pile spacing was less than 2.25D. This failure mechanism was adopted by the design code such as Specifications for highway bridges (2002) in Japan. Mano et al (1986) carried out a model test to observe the ground deformation during loading by using X-ray. They showed that some block failure occurred only in the ground where is upper two thirds of the pile and in the lower ground, a punching failure occurred. Some equation for group pile design in clayey ground was proposed based on the observation.

On the other hand, the group pile in sandy ground exhibited different behavior. Vesic (1969) showed that the group pile could carry more than the summation of single piles in sandy ground. And center pile carries more load than corner pile. This tendency could not explained by the block failure like the group pile in clayey ground. However it was unclear why the subgrade reaction became smaller and such load distribution in pile members occurred.

To investigate the difference between the group pile and a single pile or the mechanism of the interaction during group pile loading, it is effective to measure the ground deformation because the interaction occurred there. These kinds of observation were conducted previously to investigate a bearing mechanism of a single pile by using X – ray Computed Tomography (Ekisar and Otani, 2012), Magnetic Resonance Imaging (MRI) (Ng et al, 1996), Digital Image Correlation (Sadek, 2003; Yamamoto, 2001; White and Bolton, 2004). They showed how the shear strain developed around pile tips. These ground deformation contributed to developing the numerical analysis for the single pile. Hirayama (1988) suggested punching failure occurred for pile foundation and the equation based on the shear expansion theory showed good agreement with his experimental results.

For evaluating the settlement of group pile, numerical analyses were developed such as boundary element method by Poulos (1968), hybrid method by Randolph (1994) and finite elementary method. But these methods were considered only for bearing load of the group pile so it was still not clear if these methods represented the mechanism of soil-pile-soil interaction. That is because the behavior of the ground under the loading of the group pile in sandy ground has not been investigated yet.

In this study, loading tests of the group pile and single pile were conducted at first to confirm the effect of the interaction in case of the group pile with narrow spacing. Moreover test results show the occurrence of the strong effect of interaction during loading. Then visualizing tests and image analysis were conducted for the group pile and single pile to show how the ground deformed when the strong interaction occurred and to consider the mechanism of the interaction.

2. TEST APPARATUS AND TEST PROCEDURE

Group pile loading tests and visualizing tests were conducted in a large rigid soil tank as shown in Figure 1.

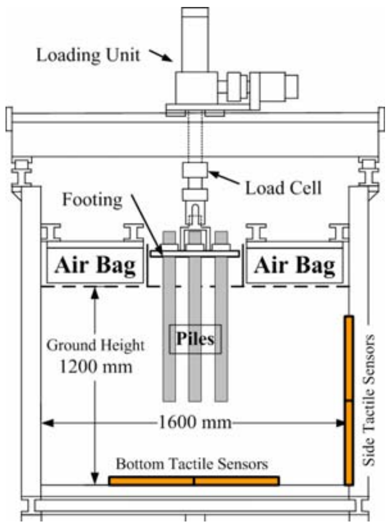

Figure 1 Cross section of test equipment

Table 1 All conducted test conditions

Case No.	Aim of Tests	Test Location	Pile shape	Pile Length	Number of piles	Spacing between Piles	Confining Pressure
1	Group pile loading tests	Center of soil tank	Cylindrical Diameter ; 40mm	1000mm	9 (3×3)	100mm (2.5D)	50kPa ⇓ 100kPa ⇓ 150kPa ⇓ 200kPa
2						200mm (5.0D)	
3	Vertical pressure distribution under group pile loading			1300mm		100mm (2.5D)	
4						200mm (5.0D)	
5	Horizontal pressure distribution under group pile loading	Near the side wall of soil tank		1000mm		100mm (2.5D)	
6						200mm (5.0D)	
7	Single pile loading test	Near the back wall of soil tank	Cylindrical Diameter ; 40mm	1000mm	1		
8		Center of soil tank	Cylindrical Diameter ; 150mm	1000mm	1		
9	Group pile Visualizing tests for image analysis	Near the front wall of soil tank	Rectangular parallelepiped Width ; 40mm × 80mm	1000mm	3	100mm (2.5D)	50,100,150,200 200,150,100,50
10						200mm (5.0D)	

Its internal dimension was 1600mm×1600mm (width) × 1200mm (depth). The frontal wall of the tank was made of a transparent acrylic plate to observe ground deformation for PIV analysis. On the wall, a Teflon sheet was placed to reduce friction between soil and sidewall. On the top of this tank, a loading unit was installed, on which a load cell was set on the lower end of that unit, to measure the total axial loading on piles. The detail of this loading unit was described by Goto et al. (2012). Air bags were placed on the surface of the model ground with the exception of the testing area, to apply the confining pressure to the ground.

All conducted test conditions are shown in Table 1. The testing locations in the table were shown in Figure 2. The test equipment was reset after every case.

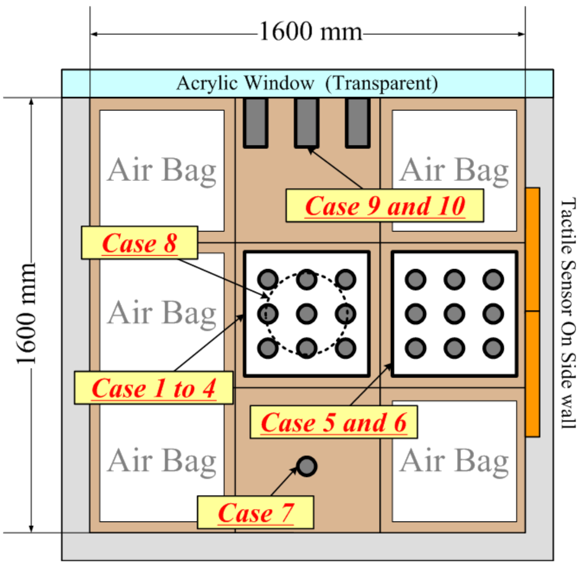

Figure 2 Test locations (top view of the soil tank)

Model piles which constituted the pile group in the loading tests; from Case 1 to Case 6, were cylindrical in shape and made of aluminum, 40 mm in outer diameter, 4 mm in thickness, and 1000 mm or 1300 mm in length. The bottom of the piles were closed by a flat plate and the strain gauges were attached inside the pile at 5 levels along the piles and each level had 4 strain gauges to measure both the axial force and bending moments in two directions.

For comparison with the group pile behavior, single pile loading tests were conducted with the same diameter of pile (Case 7); 40 mm in outer diameter, and a large diameter pile (Case 8); 150 mm in outer diameter, 10 mm in thickness and 1000 mm in length. The strain gauges were attached inside the both piles at the same location as in the constituting piles of the group pile. Moreover, the bottom of the large pile was closed by the load cell that was divided into annular 4 rings and the contact pressures were measured individually for each ring as shown in Figure 3.

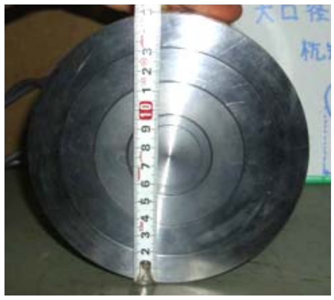

Figure 3 Annular load cells on the bottom of large pile

In the visualizing tests (Case 9 and Case 10), each model pile was rectangular parallelepiped in shape, and made of aluminum, 40 mm × 80 mm in cross section, 4 mm in thickness and 1000 mm in length. The bottom of the piles was closed by flat plates and the strain gauges were attached inside the pile at top and bottom. Each level had 4 strain gauges similar to the cylindrical model piles.

Model ground was 1200 mm in height and made of air-dried Silica Sand No.5; D50 = 0.523 mm, e_{max} = 1.09 and e_{min} = 0.66. It was constructed by sand spreading method and manual compaction at every 150 mm deposition. The total amount of sand was measured when it was poured. The relative density calculated from that weight was around 90%.

After the ground was built up below the initial height of the pile tips, the pile models were set on the ground. Each head of pile was fixed to a steel plate that is called "footing" in Figure 1 in group pile tests. After setting the piles, the ground was built again up to 1200 mm in height. Then the above-mentioned air bags were installed on the surface of the ground.

The group pile loading tests; Case 1 to Case 6, were performed with 9 cylindrical piles (3*3) at the center or near the side wall of the soil tank. Two kinds of center-to-center spacing between piles were used: 5 times (5D) and 2.5 times (2.5D) diameter of piles.

The plan view of the configuration of the pile group is shown in Figure 4. In each tests, two kinds of pile loading were employed. First was individual loading in which each pile was separated from the footing and pushed down individually while other piles did not move. Another was group pile loading in which the footing was pushed down with all piles connected to the footing, which meant all piles were pushed down together.

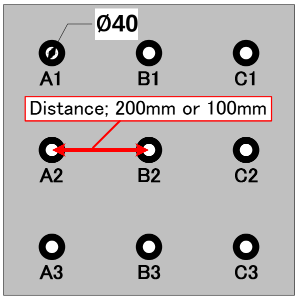

Figure 4 Pile layout of the group pile loading tests

These tests were performed in displacement - control manner; the loading rate was 2 mm/min in individual loading and was 1 mm/min in group pile loading. Both individual and group pile loadings were continued until the settlement became 30 mm under a confining pressure. For measurements of the tactile sensors, these loading processes were interrupted for several minutes at every 10 mm settlement. After that, the confining pressure was increased to the next step and the individual and group pile loading were conducted again under the condition. The confining pressure was increased from 50 kPa to 200 kPa, with 50 kPa increment as Table 1 showed.

The single pile loading tests in Case 7 and Case 8 were conducted under the same conditions of the confining pressure; 50 to 200 kPa, and the loading rate; 2mm/min, with the group pile loading tests. For measurements of the tactile sensors, these loading processes were also interrupted for several minutes at every 10 mm settlement of piles.

The group pile visualizing test; Case 9 and Case 10 were performed with 3 rectangular parallelepiped piles behind the transparent front wall (Figure 5). These tests reproduced a 2-dimentional model of a group pile and two kinds of center to center spacing were used such as the group pile; 5times (5D) and 2.5 times (2.5D) diameter of the pile. The plan view of the configuration of the pile group is shown in Figure 5. In both condition of the visualizing tests, only group pile loading tests were carried out under each confining pressure, by increasing that pressure (50, 100, 150 and 200 kPa).

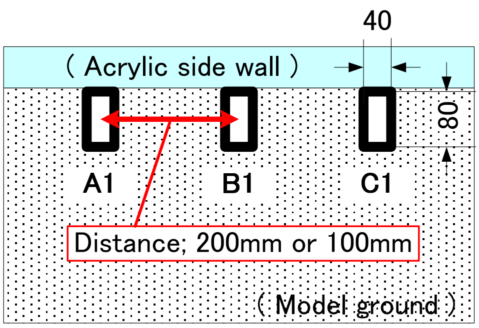

Figure 5 Top view of the group pile visualizing tests

3. BEHAVIOR OF PILES UNDER THE GROUP PILE LOADING TEST

3.1 Yielding point of the bearing load

Figure 6 shows the relationships between total bearing load measured by load cell and settlement during the group pile loading phase in Case 1 and Case 2. The load-settlement curves were classified and presented by confining pressures in all cases. All the yielding points of the curves were marked by arrows in the figure. The settlement at yielding points with 2.5D pile spacing are greater than that of 5.0D pile spacing under each confining pressure.

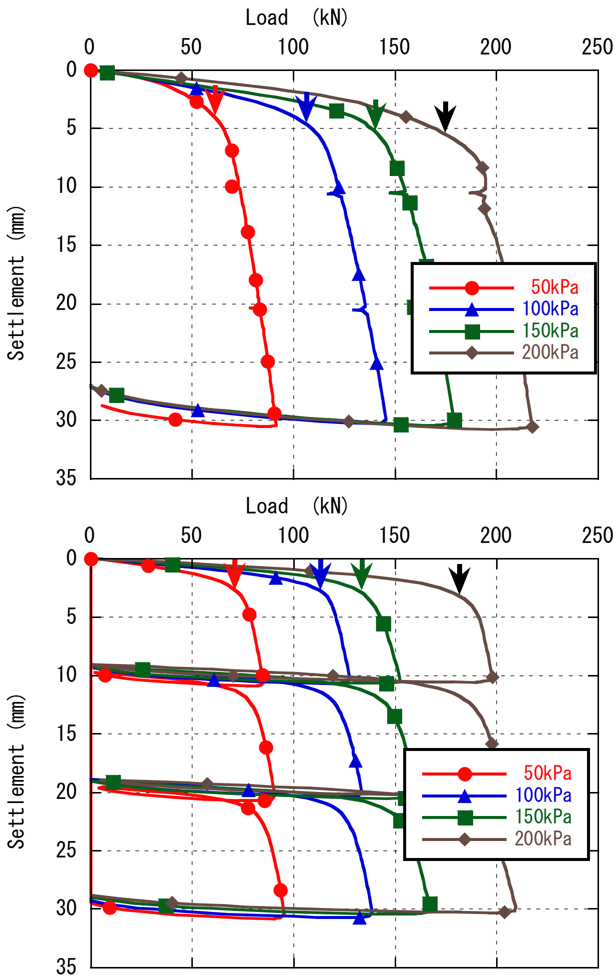

Figure 6 Load-settlement curves in Case1 and Case2

Figure 7 shows the load-settlement curves during the group pile loading tests at the confining pressure of 100kPa in Case 1 and Case 2. The results of single pile loading test with the same diameter pile in Case 7 and the single pile loading test with large diameter pile in Case 8 under the same confining pressure were also plotted and compared in this figure. Load of the single pile with the same diameter in this figure was multiplied by nine, which is the number of piles, for comparison. The yielding points of the single pile tests were also marked by arrows in the figure.

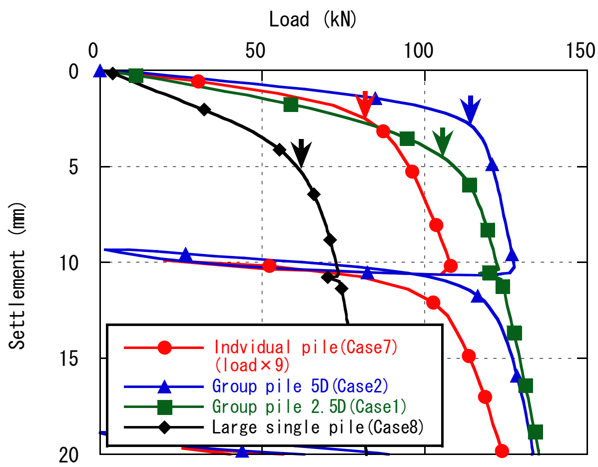

Figure 7 Yielding point of group pile, individual pile and large single pile at 100kPa confining pressure

A comparison of single pile loadings with larger (Case 8) and smaller (Case 7) diameter suggested that settlements at the yielding point became much greater when the diameter of the pile increased as shown in Fig.7.

For the group pile loading tests, settlement at yielding with 5D pile spacing (Case 2) was almost identical with that of the small single pile (Case7) as shown in Figure 7. On the other hand, the yielding settlement with 2.5D spacing (Case 1) became greater than 5.0D. The tendency that yielding settlement increases with pile spacing decreasing was similar to the observation with changing diameter of single pile.

The tangential lines of the load-settlement curve on initial and after yielding part were plotted in Figure 8. It shows that initial stiffness becomes smaller with narrower pile spacing. On the other hand, the behavior after the load-settlement curves are yielded these tendencies would be explained later relating with ground deformations.

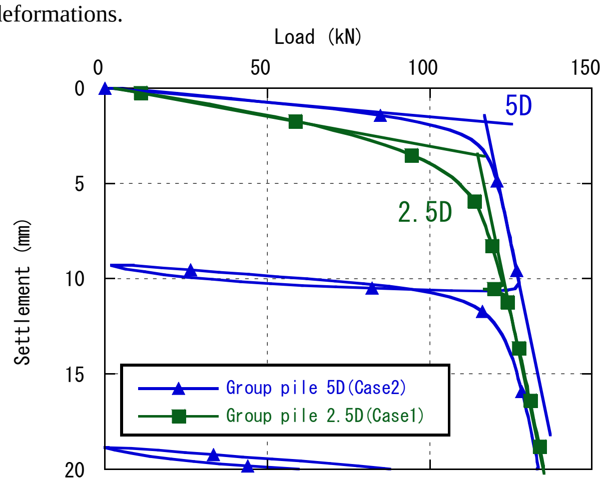

Figure 8 Tangential lines on load settlement curve on initial and after yielding of group pile at 100kPa confining pressure

3.2 Load distribution between each pile

Figure 9 shows the mean tip resistance changing with the location of pile – central, central of outer line, and corner, normalized by the total mean tip resistance under the confining pressure of 50kPa (Case 1 and Case 2). With the wider spacing, the ratio of each pile was almost equal to unity throughout the loading. It suggests that each pile behaved independently and that the interaction was insignificant. In contrast, for narrower spacing, the ratio changed with the penetration. The load concentration shifts from corner piles to center piles.

Figure 10 shows the tip resistance changing with the location on the bottom of the large pile (Case 8), normalized by the total mean tip resistance. This tip resistance distribution was measured by annular load cells which were installed at the bottom of large pile. The stress concentration also shifts from the edge to the center of the pile. This finding suggests that the significant interaction occurs for narrower spacing and these piles behave as one large block. For details, refer to Goto et al (2012).

4. BEHAVIOR OF MODEL GROUND

To further understand the mechanism of pile-to-pile interaction, it is necessary to observe the ground behavior during the group pile loading.

4.1 Soil Pressure Distribution

4.1.1 Tactile sensors

The tactile sensor manufactured by Nitta Corp. were installed both at the bottom and the side wall of the soil tank. The advantage of this sensor is the ability to measure the distribution of normal pressure. Although earth pressure transducer is often used, the device cannot demonstrate the stress distribution and hence, is not relevant for the present research purpose, to discuss the effect of group pile on the stress transfer.

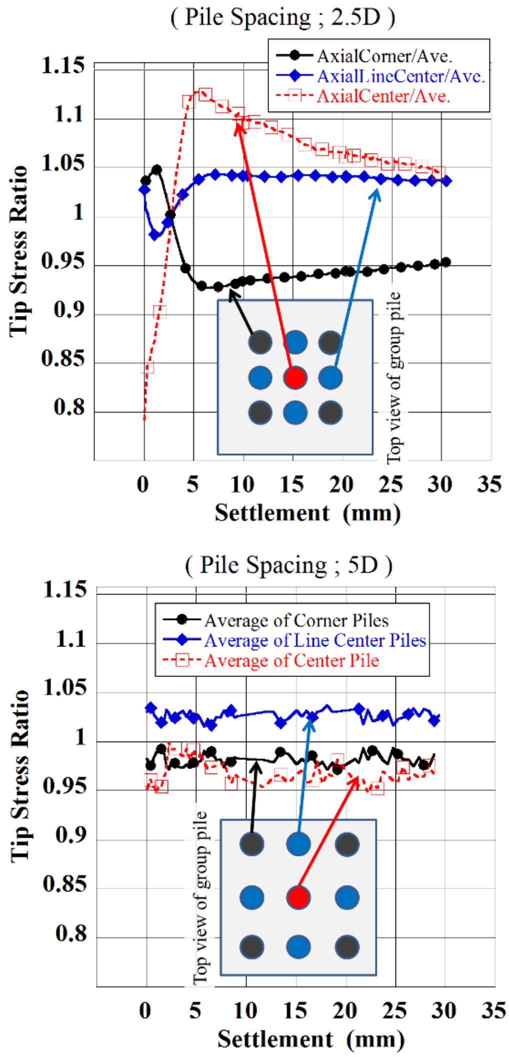

Figure 9 Tip resistance ratio among individual piles

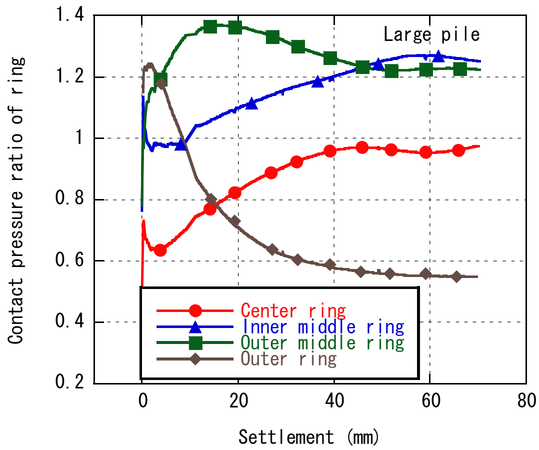

Figure 10 Tip resistance distribution of a single pile with large diameter at 50kPa confining pressure

The sensor consists of two thin PET sheets and the inner side of each PET sheet contains rows and columns of resistive ink. At the point of grid, where rows and columns of the ink overlap, the applied forces are measured as the change of the electric resistance between rows and columns of ink. The sensor sheet covered 440 mm × 480 mm area, containing 44 rows and 48 columns of ink resulting in 2016 sensing cells spaced at 10 mm at centers in each direction. The system of tactile sensors includes this sheet sensor, a connecter and software as Figure 11 shows. The connecter reads the resistance value consecutively from the sensor sheet and the pressure distribution is calculated by the program as Figure 12 shows. In this example of the pressure distribution, the red part means higher pressure and the blue part the lower. The original data to show the pressure distribution has the definite pressure value at each sensing points. By changing the connecter, the data of pressure distribution are gained from several sheets and these data are synthesized by the supplied software.

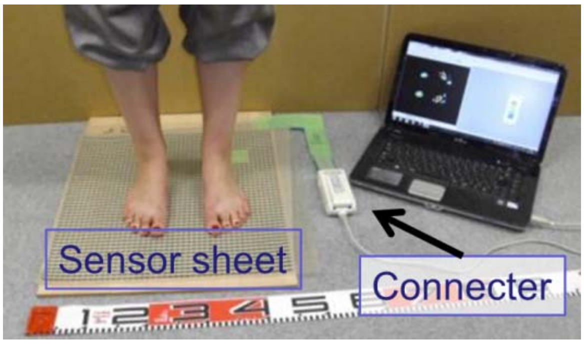

Figure 11 The tactile sensor system

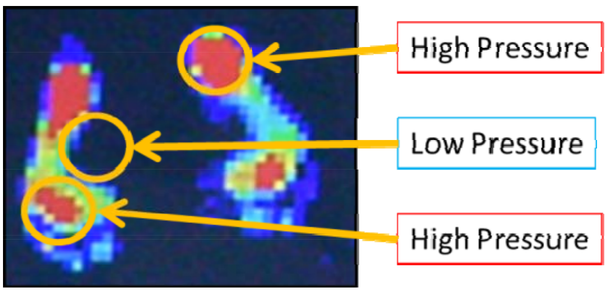

Figure 12 Example of measured pressure distribution by a tactile sensor

4.1.2 Vertical pressure distributions

Figure 13 shows the representative distribution of normal pressure at the bottom of the soil tank measured by tactile sensors (Case 3 and Case 4). The pressure value in the figure is the difference between pre- and post-loading conditions. “Distance” in the figure means the distance from the pile tips to the tactile sensor at the bottom when the pressure was measured as Figure 14 shows.

The pressure distribution would be classified into 3 types by the distance. First, when the distance between pile tips and the sensors at the bottom is large enough; more than 290 mm in both test cases, the higher pressure (red color) occurred below the central pile and the pressure decreased concentrically in the radial direction (becoming blue) for both narrower and wider spaces. Second, with distance becoming smaller, the maximum pressure shifted to the zones between piles and formed a ring distribution. The pressure below the central pile did not achieve the maximum. This distribution also arose in both narrower and wider space group pile loading tests. Third, with distance becoming even smaller, the distribution changed only in case of wider spacing. The high pressure area is located just under the piles separately. On the other hand, the stress distribution under narrower spacing kept the ring distribution at this distance.

These changing of the vertical pressure distributions under group pile loading were detected for the first time by measuring with the tactile sensors. This distribution reveals the effects of the interaction in the ground under group pile loading. Therefore, these 3 kinds of distribution were compared with elastic solutions. The elastic solution was calculated by setting 9 loading points in a homogeneous elastic half-space. The measured tip load was applied with the calculations. Figure 15 shows the calculated pressure distribution at several distances from the pile tips.

First concentrically distribution and third separated distribution were good fit with the elastic solution. On the other hand second ring pressure distribution were never represented by these 2 simulated distributions

The incompatibility of the real pressure distribution with the two kinds of simulation suggests that the interaction of each pile would be strong in this area where ring pressure distribution profile showed.

Because the 5.0D spacing pile group also shows the ring pressure distribution as well, the wider group spacing generated the interaction of piles. This consideration is different from the observation based on the bearing load or tips stress distribution among piles.

One of the reasons for this difference may be the location of the area where this ring pressure distribution occurs. In case of wider spacing, the ring pressure distribution occurred at a distance from the pile tips. That is why the interaction in the ground would not affect the bearing capacity or tip resistance distribution of the wider spacing. In contrast, the ring distribution occurred near the pile tips in case of narrow spacing. This would affect the behavior of the piles; as a result, the yielding point was different from the superposition of the single pile loading (Figure 7) and the tip stress distribution showed the changing with distance as shown in Figure 9.

4.1.3 Horizontal pressure distributions

The horizontal pressure distribution was measured by tactile sensors placed on the side wall when group pile loading tests were conducted near the side wall (Case 5 and Case 6) as Figure 16 shows. The side wall was 90 mm away from the center of the nearest pile in a group. Figure 16 shows the horizontal pressure distribution at the confining pressure of 100 kPa. The pressure value is also the difference between pre- and post-loading conditions. The locations of the piles are shown by red line in the figure.

In case of the wider spacing pile group, higher pressure occurred under each pile separately and the shape of each distribution was concentric. The highest pressure in each distribution occurred around 90 mm below the pile tips. This suggests that the highest pressure occurred around 45 degrees obliquely downward from the pile tip. This profile is compatible with the summation of the results measured during the individual loading tests or the elastic solutions calculated by elastic solution.

On the other hand, in case of 2.5D spacing pile group, a clumpy distribution was observed. This would support the point that the narrow spacing behave as one block because of the higher interaction among piles. Moreover, it was detected that the pressure changed area propagated downward in narrow spacing group pile as shown in Figure 17. This insists that the effective area of the ground below the piles would expand because of the interaction of piles. It would cause the larger deformation of the ground below the piles in narrow spacing group pile. That is why the settlement stiffness in narrower spacing pile group would decrease in elastic phase as shown in Figure 7.

4.2 Soil Movement (Visualizing tests and PIV analysis)

The significant interaction in a group pile with narrow spacing was also studied from the viewpoint of ground deformation.

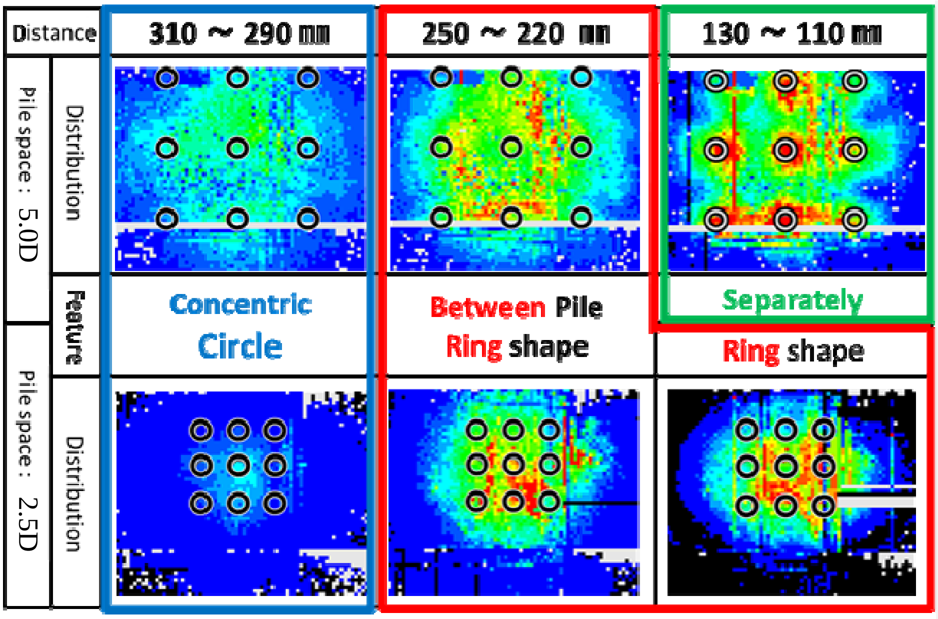

Figure 13 The vertical pressure distribution on the bottom of the soil tank

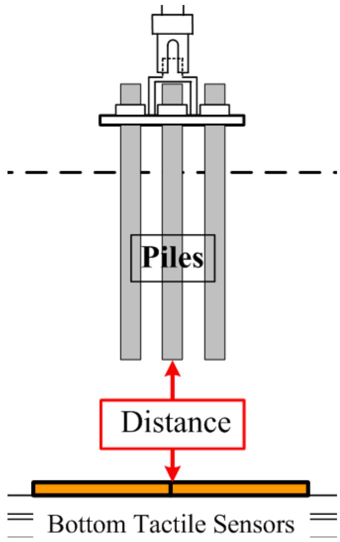

Figure 14 The distance from the pile tips to the tactile sensors

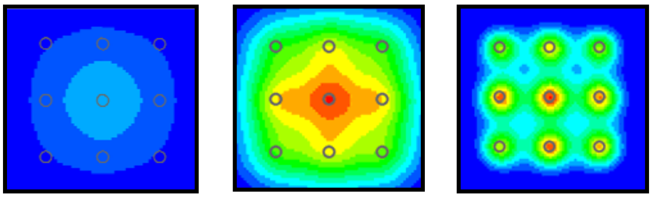

1) distance; 290mm 2) distance; 220mm 3) distance; 110mm
a) in 5.0D Group Pile

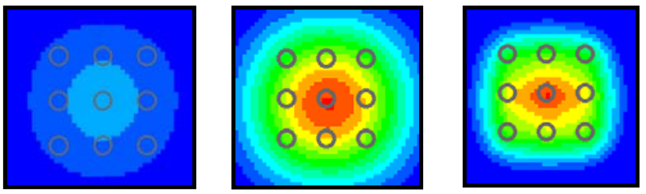

1) distance; 290mm 2) distance; 220mm 3) distance; 110mm
a) in 2.5D Group Pile

Figure 15 Elastic solution of pressure distribution

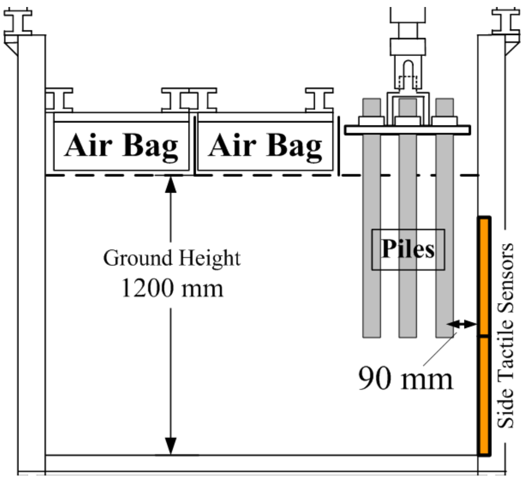

Figure 16 Cross section of test equipment in Case 5 and Case 6

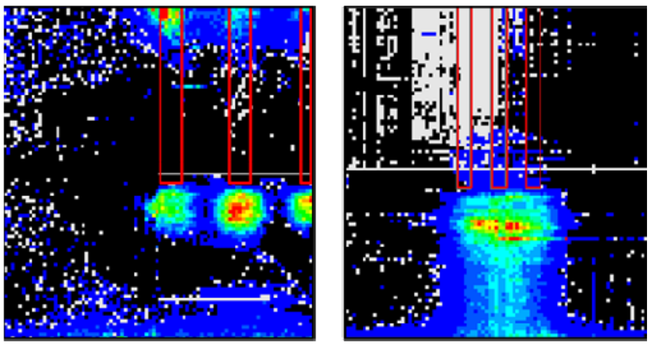

Figure 17 Tip horizontal pressure distribution under group pile loading

Figure 18 shows the ground deformation after loading tests in Case 1 and Case 2. The dotted lines in the figures show the initial positions of each colored sand layer before loading tests. In case of the group pile with wider space, the colored sand layers deformed below the each pile tip separately. In contrast, in case of narrow space, the ground below the pile tips deformed in a contiguous concave way and the ground between the piles also deformed downward. These different shapes of the ground deformation according to the pile space suggest that the group pile with narrow space affected the ground as one block because of the interaction between piles.

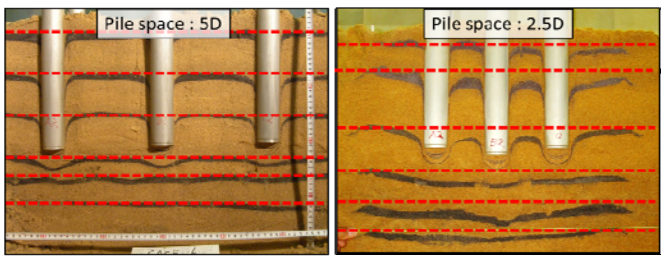

Figure 18 The ground deformation after the loading tests in Case 2 and Case 1

To further study this effect of the interaction on the ground deformation, real-time observation of the ground deformation through a transparent acrylic wall was conducted as shown in Figure 19. The group pile was simulated as the 2-D model in this visualizing tests, by using three rectangular piles as shown in Figure 5. Colored sand layers were installed in the ground below the pile tips every 40 mm and the thickness of each layer was 20 mm. The progress of the deformation was recorded by two digital cameras; Nikon D60. The records were taken at every 5 seconds automatically by the software; Nikon Camera Control Pro 2. One camera recorded the whole ground deformation. Another one zoomed in on the area below the pile tip; about 300 mm in width and 200 mm in height, by using a 200 mm telephoto lens. Two lights were installed to exclude shadows from the observation area.

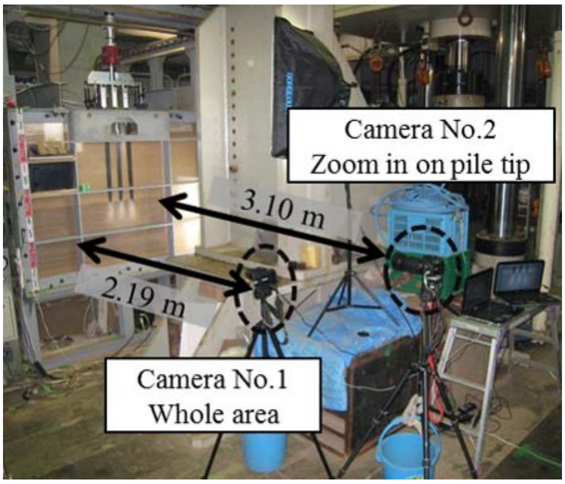

Figure 19 Observation system of the real-time ground deformation

To analyze this real-time deformation quantitatively, the PIV analysis was applied to these pictures by using GeoPIV (White et al., 2003). Figure 20 shows the relationship between the averaged axial strain at the pile tips measured by the strain gauges inside the piles and settlement during the group pile loading under the confining pressure of 100 kPa. The result was split into 4 phases; 1-Elastic, 2-Before Yielding Point, 3-After Yielding Point, and 4-Plastic. The PIV analysis was applied for each phase individually. The analysis conditions for PIV are shown in Table 2.

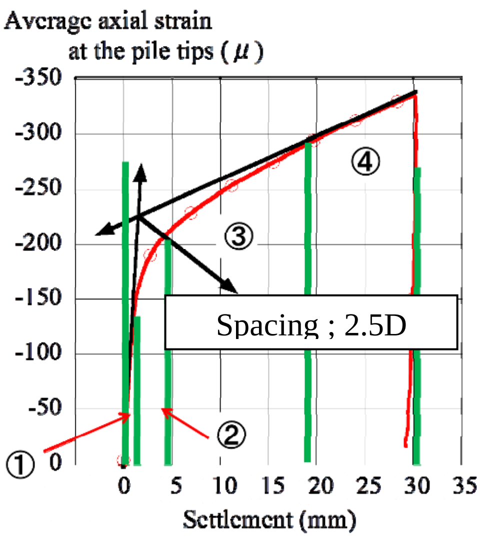

Figure 20 The four phases for PIV analysis

Table 2 The analysis conditions of PIV analysis

The size of the target mesh	24	pixel
Space between target mesh	8	pixel
Search range	250	pixel
Time interval between pictures	20	sec

Figures 21 and 22 show the typical result of PIV analysis of the ground deformation in the group piles with 2.5D and 5.0D pile spacing which settled down from 0 to 30 mm in the first loading. The solid square indicates the location of the piles. A vector was just connecting the locations of each mesh before and after 30 mm settlement of the pile.

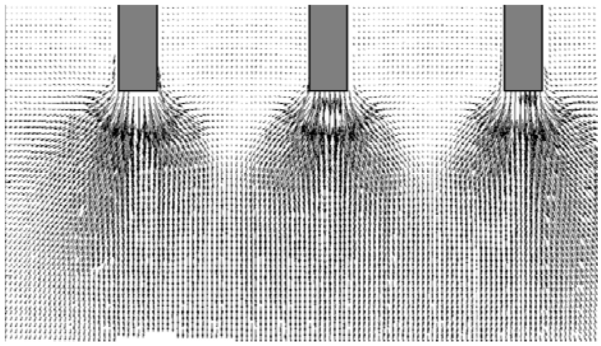

Figure 21 Distribution of the ground deformation during 0 to 30 mm settlement in 5.0D group pile (Case 10)

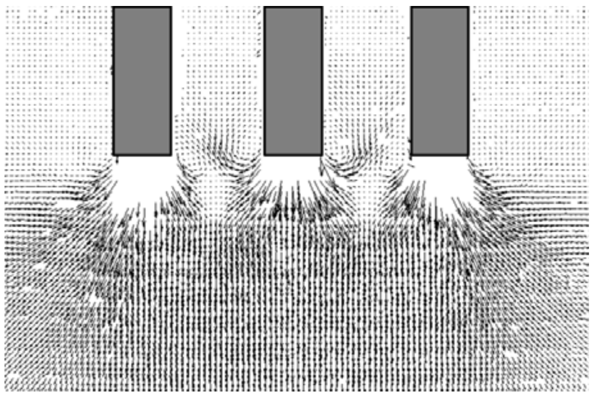

Figure 22 Distribution of the ground deformation during 0 to 30 mm settlement in 2.5D group pile (Case 9)

The deformation near each pile tip showed the pattern of the punching failure in the case of 5.0D group pile and the distribution is consistent with the result of the single pile by White (2007). Boundaries between deformation and non-deformation were observed at 45 degrees from each pile tip. However, the slanted downward vectors from two piles collided horizontally at the point where in the center pile was and vertically at 2.5D lower than pile tip. The horizontal component was canceled after the collision, and only vertical components remained. It suggested that an interaction occurred in the ground even though the spacing of the pile group was 5.0D. But the behavior of the bearing load was similar to the summation of the single pile and showed the less effects of the pile-soil-pile interaction in the author's previous studies (Aoyama et al. 2012 etc.). This reason would be discussed later by considering the increment of the deformation of every pile settlements.

In case of 2.5D group pile, the position where the collision of slanted vectors occurred near to the pile tips, around 1.5D below the elevation of the pile tips. As a result, a clear block area with vectors with only vertical component spread below the group pile. However, on the outer side of the group pile, the distribution of the deformation was almost the same as the distribution in 5.0D group pile. The angle of the boundary between deformation and non-deformation was also 45 degrees. This suggested that the intensity of the effect by the interaction differed according to location of the pile and this corresponded to the results of the loading tests.

To discuss the effect of the settlement against the distribution of the ground deformation, two kinds of ground deformations were compared. One is the ground deformation while the settlement of the pile is between 0 to 1 mm. By the settlement, the tip resistance did not yield and the relationship between the tip resistance and the settlement was almost linear. The other was the ground deformation while the settlement of the pile went from 9 to 10 mm. During the settlement, the tip resistance was already yielded.

Figure 23 shows the contour of the increments about the vertical components of the ground deformation from 0 to 1 and from 9 to 10 mm settlement in case of 5.0D pile spacing. The peak of vertical displacement occurred below each pile tips individually and uniformly. The shape of peak was like a cone. The distribution did not change by increasing the settlements of the pile or the hysteresis of the loading.

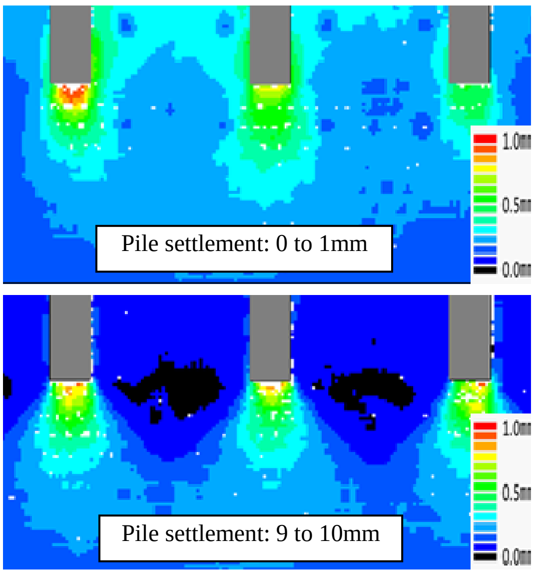

Figure 23 Distribution of the increment of the vertical displacement in 5.0D group pile (Case 10)

On the other hand, the peak of the displacement was not observed below each pile tip individually until 1 mm settlement in case of the 2.5D group pile as shown in Figure 24. The distribution of the vertical displacement showed a block below the group pile. However, the peak of the vertical displacement was observed below each pile tip individually during the settlement from 9 to 10 mm. The block distribution that developed just below the pile tips disappeared even though a continuous distribution was observed at 1.5D distance bellow the pile tips.

Figure 25 shows the distribution of the vertical displacement along the same elevations as in the case of single pile. The displacement was observed during pile settlement from 0 to 1 mm. The shown elevation was every 0.5D below the pile tips.

Figure 26 shows the comparison of the vertical displacement of ground between 5.0D group pile and the summation of the single pile. Regardless the settlement of the pile, both curves fitted each other. This showed the deformation of the ground under the 5.0D group pile loading could be represented by just summation of the single pile. It suggested less effect of the interaction occurred in the ground in case of the 5.0D group pile.

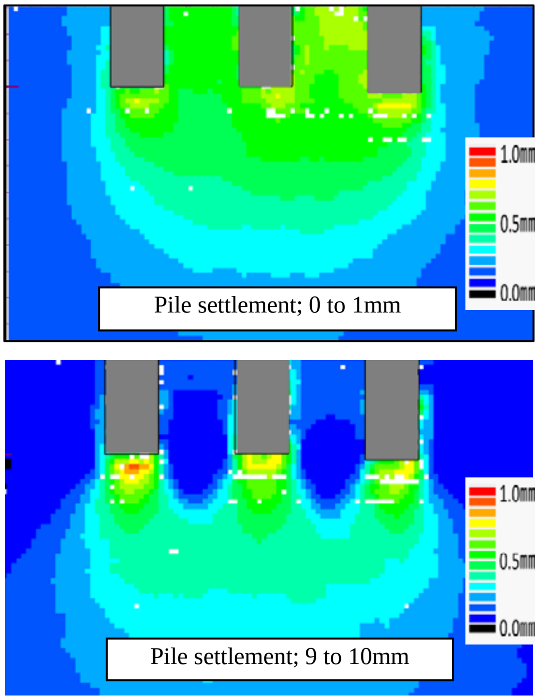

Figure 24 Distribution of the increment of the vertical displacement in 2.5D group pile (Case 9)

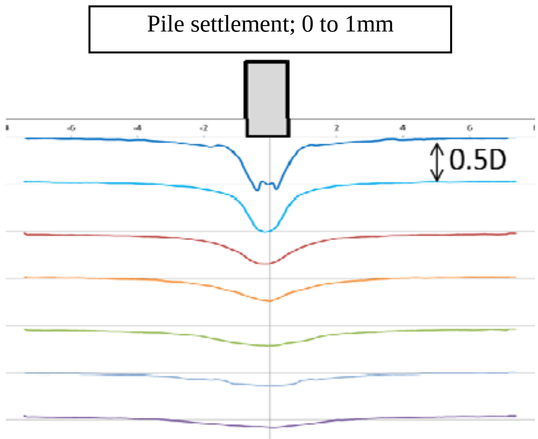

Figure 25 Distribution of the increment of the vertical displacement at every 0.5D depth in single pile

On the other hand, in 2.5D group pile, some difference from the summation of the single pile was observed as shown in Figure 27. Larger displacement in the area below the piles was clearer for the comparison during the settlement from 0 to 1 mm.

In addition, the vertical settlement in the group pile became larger than the summation of the single pile on the area which was 2 to 3D below than the pile tip. This was a proof that a particular interaction for the group pile occurred in the area because of overlapping of the stress caused by plural piles in the ground. Such larger settlement in 2.5D group pile would cause the smaller increment of tip resistance before the tip resistance yielded, as shown in Figure 8.

However, both curves of the group pile and the summation of single pile fit well during the settlement from 9 to 10 mm even in the case of 2.5D group pile. It meant the additional effect of the interaction did not develop during the settlement from 9 to 10 mm; after the tip resistance yielded.

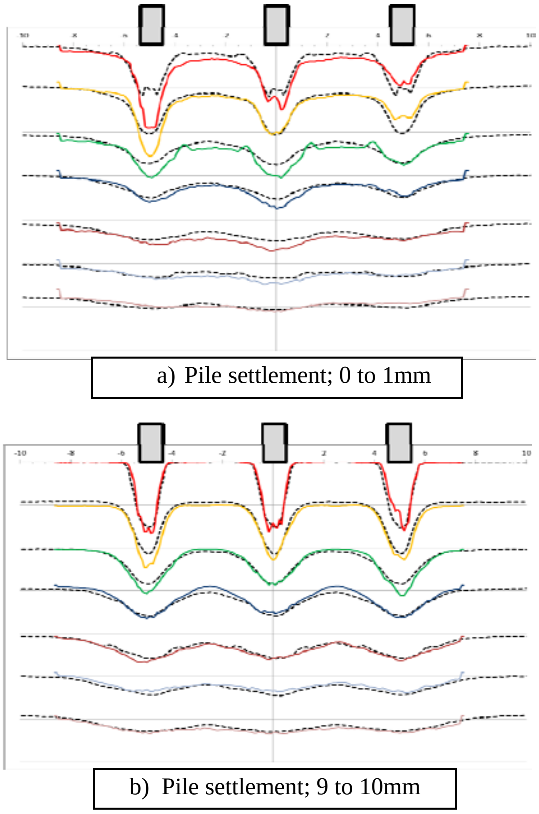

a) Pile settlement; 0 to 1mm

b) Pile settlement; 9 to 10mm

Figure 26 Vertical displacement comparison between the group pile and summation of single pile in 5.0D group pile

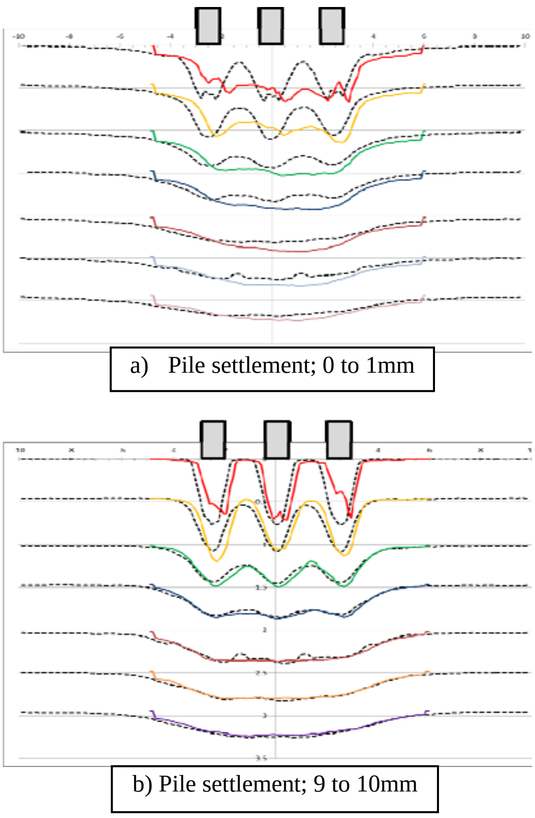

a) Pile settlement; 0 to 1mm

b) Pile settlement; 9 to 10mm

Figure 27 Vertical displacement comparison between the group pile and summation of single pile in 2.5D group pile

5. CONCLUSION

Vertical loading tests of a pile group and visualizing tests were conducted in sand. After comparing the bearing load and distribution of tip load among piles, the vertical and lateral pressure distribution and the ground deformation between two kinds of pile spacing: 5D and 2.5D, the following conclusions may be drawn.

1) For 2.5D pile spacing, a group pile yields at a larger displacement and the apportionment of tip resistance among piles changed depending on the penetration length. These behaviours are consistent with that of large diameter pile. This suggests that 2.5D group pile works as one block.
2) Ring distribution was observed in the vertical pressure recorded by the tactile sensors. This form was not represented by elastic calculation this suggested some interaction occurred. It affects the behaviour of a pile group as one block, if it occurred near the pile tip in case of the narrow spacing group pile.
3) A clumpy distribution was observed below the piles by the tactile sensors on the side wall in 2.5D group pile. This supports the point that 2.5D group pile works as one block. Furthermore, the downward propagation of lateral pressure distribution was also measured in wider area at the narrow space. This suggests the large deformation under the same penetration length and the settlement stiffness will decrease in 2.5D spacing.
4) The consecutive ground deformation in a block way occurred in the elastic phase only in case of 2.5D group pile. The interference of ground deformation affected the behaviour of the group pile because the distance from the pile tips to the area was short enough.

ACKNOWLEDGEMENT

Authors are gratitude to Dr. Sadao Yabuuchi, President of Japan Pile Corporation for his invaluable support. Authors also appreciate to members of the pile group committee of Kanto Branch of JGS for their advice. PIV program used in this study was developed by Prof. David J. White of University of Western Australia. The authors express the sincere gratitude to the supports mentioned above.

6. REFERENCES

Aoyama, S., Goto, S. Liu, B., AyalaAlarco, R., Takita, A. and Towhata, I., (2012) “Bearing mechanism and the interaction between piles and soil under group pile loading”, Proceedings of IS-Kanazawa 2012, pp519-526

BCP Committee, (1971) “Field tests on piles in sand”, Soils and Foundations, Vol.11, No.2, pp29-49,

Ekisar, T., Otani, J., Hironaka, J., (2012) “Visualization of soil arching on reinforced embankment with rigid pile foundation using X-ray CT”, Geotextiles and Geomembranes 32, Elsevier, pp44 – 54

Endo T., Yamaguchi K., Nomura N. (1980), “The Plate bearing tests on the multicolumn-type foundation in Ohnaruto bridge”, Tuchi to Kiso, November, Vol. 28, No.11, pp43-48

Goto, S. Aoyama, S., Liu, B., AyalaAlarco, R., Takita, A. and Towhata, I., (2012) “Model pile and pile group bearing capacity in large scale soil tank test”, Proceedings of IS-Kanazawa 2012, pp511-517

Hirayama, H., (1988), “A unified base bearing capacity formula for piles”, Soils and Foundations, Vol. 28, No. 3, pp91-102

Japan Road Association (2002), Specifications for highway bridges, Vol.4

Mano, H., Uchimura, H. and Kishida, H., (1986) “The Bearing Capacity of Pile Group on Soft Clayer Soil, Proceedings of N0.21 Annual conference of JGS, pp.1195-1196, (in Japanese).

Ng, T.-T., Kelley, M., and Sampson, J., (1996) “MRI studies of direct shear tests on round particles”, Proc., 11th Conf. of ASCE, Engineering Mechanics Div., ASCE, Reston, Va., pp572–575

Poulos, H.G., (1968) “Analysis of the settlement of pile groups”, Geotechnique, Vol. 18, pp449-471

Randolph, M.F, (1994) “Design methods for pile groups and piled rafts”, Proc. 13th SCSMFE, New Delhi, Vol. 5, pp61-82

Sadek, S., Iskander, M.G., Liu, J., (2003) “Accuracy of Digital Image Correlation for Measuring Deformations in Transparent Media”, Journal of Computing in Civil Engineering, Vol. 17, No. 2, pp88-96

Yu, Ching-Han, (2011) “On Design and Construction of Pile Group Foundation of Taipei 101”, Geotechnical Engineering Journal of the SEAGS & AGSSEA, Vol.42 No.2, pp56-69

Vesic, A.S., (1965) “Ultimate Loads and Settlements of Deep Foundations in Sand”, Symposium on Bearing Capacity and Settlement of Foundations, Duke University,

Vesic A.S., (1967) “A Study of Bearing Capacity of Deep Foundations”, Final Rep., Project B-139, Georogia Inst. of Tech.

Vesic A.S., (1969) “Experiments with Instrumented Pile Groups in Sand, Performance of Deep Foundations”, ASTM STP 444, American Society for Testing and Materials, pp177-222

Whitaker, T., (1957) “Experiments with Model Piles in Groups, Geotechnique, Vol. 7, pp147-167

White D.J., Take W.A. and Bolton M.D., (2003) “Soil deformation measurement using particle image velocimetry and photogrammetry”, Geotechnique Vol.53, No.7, pp619-631

White, D. J., Bolton, M. D., (2004) “Displacement and strain paths during plane – strain model pile installation in sand”, Géotechnique 54, No. 6, pp375 – 397

Yamamoto, K., Kusuda, K., (2001), “Failure mechanisms and bearing capacities of reinforced foundations”, Geotextiles and Geomembranes 19, Elsevier, pp.127-162